Emergence of Coherent Magnetic Excitations in the High Temperature Underdoped $La_{2-x}Sr_xCuO_4$ Superconductor at Low Temperatures

O. J. Lipscombe,[1] B. Vignolle,[1] T. G. Perring,[2] C. D. Frost,[2] and S. M. Hayden[1]

[1]*H. H. Wills Physics Laboratory, University of Bristol, Tyndall Avenue, Bristol, BS8 1TL, United Kingdom*
[2]*ISIS Facility, Rutherford Appleton Laboratory, Chilton, Didcot, Oxfordshire OX11 0QX, United Kingdom*

(Received 26 August 2008; published 22 April 2009)

We use inelastic neutron scattering to measure the magnetic excitations in underdoped $La_{2-x}Sr_xCuO_4$ ($x = 0.085$, $T_c = 22$ K) for large energy ($5 < E < 200$ meV) and temperature ($5 < T < 300$ K) ranges. At low T, the response is highly structured in E and $\mathbf{q}$, with peaks in the local susceptibility at 15 and 50 meV and a four-peaked structure in $\mathbf{q}$ for $E \approx 185$ meV. Raising T from 30 K $\gtrsim T_c$ to 300 K causes the structure in $\chi''(\mathbf{q}, \omega)$ present for $E < 70$ meV to disappear. It is replaced with a strongly damped response. We attribute this change to the disappearance of the pseudogap with increasing temperature.

DOI: 10.1103/PhysRevLett.102.167002 PACS numbers: 74.72.Dn, 74.20.Mn, 75.40.Gb, 78.70.Nx

In addition to their high transition temperatures, the cuprate superconductors have many intriguing properties. In the underdoped and superconducting region of the phase diagram, the electronic excitations show an unusual loss of low-energy spectral weight as T is lowered. This starts well above T_c. The phenomenon is observed in many electronic properties [1,2] including angle resolved photoemission spectroscopy (ARPES), Raman spectroscopy, optical conductivity and scanning tunneling microscopy (STM). It can be described phenologically in terms of a partial- or pseudo- electronic gap. The superconducting state gap emerges from the normal state pseudogap (PG) over much of the cuprate phase diagram and many believe that the pseudogap is key to understanding the high-T_c mechanism.

Here we investigate the evolution of the spin dynamics of an underdoped superconductor over the E and T ranges where the charge excitations show their biggest changes. Specifically, we have made high-resolution inelastic neutron scattering (INS) measurements of the collective spin excitations in $La_{2-x}Sr_xCuO_4$ (LSCO), $x = 0.085$. Measurements have been made over substantially wider ranges in energy ($5 < E < 200$ meV) and temperature ($5 < T < 300$ K) than previous studies [3–6] and reveal new structure. At low temperatures ($T \leq 30$ K), we observe peaks in $\chi''(\omega)$ at 15 and 50 meV. In addition, we find that the four-peaked structure of $\chi''(\mathbf{q}, \omega)$ in $\mathbf{q}$ rotates by $\pi/4$ between low energies (≈ 10 meV) and high energies (≈ 185 meV) and is well developed at high energies. On warming the sample from $T = 30$ to 300 K, we find that for $E < 70$ meV response becomes strongly damped and the structure observed at low T disappears.

Four single crystals with a total mass of 40.5 g were coaligned with a total mosaic of 1.5°. The crystals were grown by a traveling-solvent floating-zone technique [7] and annealed with 1 bar of oxygen for one week at 800 °C. The Sr stoichiometry was measured with SEM-EDX and ICP-AES to be $x = 0.085 \pm 0.005$. Magnetization measurements indicate that T_c(onset) = 22 K. INS experiments were performed on the MAPS instrument at the ISIS spallation source. MAPS is a low-background direct-geometry time-of-flight chopper spectrometer with position-sensitive detectors. It produces high-resolution spectra of $\chi''(\omega)$ over a wide E range which are difficult to obtain by other means [8,9]. The present experiment is the first reported application of this spectrometer to underdoped $La_{2-x}Sr_xCuO_4$.

INS probes the E and $\mathbf{q}$ dependence of $\chi''(\mathbf{q}, \omega)$. The magnetic cross section is given by

$$\frac{d^2\sigma}{d\Omega dE} = \frac{2(\gamma r_e)^2}{\pi g^2 \mu_B^2} \frac{k_f}{k_i} |F(\mathbf{Q})|^2 \frac{\chi''(\mathbf{q}, \hbar\omega)}{1 - \exp(-\hbar\omega/kT)}, \quad (1)$$

where $(\gamma r_e)^2 = 0.2905$ barn sr^{-1}, $\mathbf{k}_i$ and $\mathbf{k}_f$ are the incident and final neutron wave vectors and $|F(\mathbf{Q})|^2$ is the anisotropic magnetic form factor for a Cu^{2+} $d_{x^2-y^2}$ orbital. Data were placed on an absolute scale using a vanadium standard. We use the reciprocal lattice of the high-temperature tetragonal structure of $La_{2-x}Sr_xCuO_4$ to label wave vectors $\mathbf{Q} = h\mathbf{a}^\star + k\mathbf{b}^\star + l\mathbf{c}^\star$ and usually quote only (h, k). In this notation, La_2CuO_4 exhibits antiferromagnetic order with an ordering vector of (1/2, 1/2). In order to identify and minimize phonon contamination of our results, we collected data for six different E_i's and utilized the procedure developed in Ref. [10].

Figure 1 shows typical $\mathbf{q}$-dependent images of $\chi''(\mathbf{q}, \omega)$ for various energies and temperatures. We first consider the response in the superconducting state. At low energy, $E = 11$ meV, and temperature, $T = 5$ K [Fig. 1(a)], we observe the well-known four-peaked structure in $\mathbf{q}$ [11], with $\chi''(\mathbf{q}, \omega)$ peaked at the incommensurate positions $(1/2, 1/2 \pm \delta)$ and $(1/2 \pm \delta, 1/2)$. As for optimally doped LSCO, the excitations disperse strongly with E [9]. For $E = 50$ meV [Fig. 1(b)], they are peaked at (1/2, 1/2) and at $E = 140$ meV [Fig. 1(c)] and 185 meV [Fig. 1(d)] they are peaked at $(1/2 \pm \delta/\sqrt{2}, 1/2 \pm \delta/\sqrt{2})$ and $(1/2 \pm \delta/\sqrt{2}, 1/2 \mp \delta/\sqrt{2})$. Figure 2 shows cuts through the data in Fig. 1.

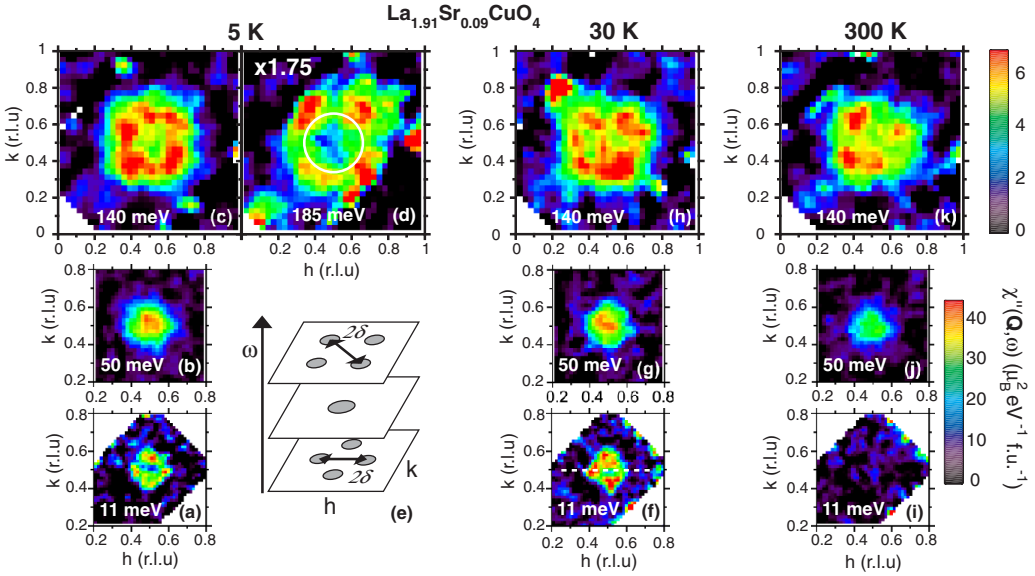

FIG. 1 (color online). Constant-E slices of data converted to $\chi''(\mathbf{q}, \omega)$ using Eq. (1). (a)–(d) at 5 K, (f)–(h) at 30 K, and (i)–(k) at 300 K. Ranges of integration were 11 ± 1, 50 ± 5, 140 ± 10 and 185 ± 15 meV, using $E_i = 55$, 240, 240, 240 meV, respectively. (e) Schematic evolution of the pattern with E. The white circle in (d) is the spin-wave pole for La_2CuO_4 for 185 meV.

In order to make a quantitative analysis of our data, we fitted 2D slices, such as those in Fig. 1, to a modified Lorentzian function [9]:

$$\chi''(\mathbf{q}, \omega) = \chi_\delta(\omega) \frac{\kappa^4(\omega)}{[\kappa^2(\omega) + R(\mathbf{q})]^2} \qquad (2)$$

with

$$R(\mathbf{q}) = \frac{[(h - \frac{1}{2})^2 + (k - \frac{1}{2})^2 - \delta^2]^2 + \lambda(h - \frac{1}{2})^2(k - \frac{1}{2})^2}{4\delta^2},$$

where the position of the four peaks is determined by δ, κ is an inverse correlation length (peak width), and λ controls the shape of the pattern ($\lambda = 4$ yields four distinct peaks and $\lambda = 0$ a pattern with circular symmetry [9]). At higher energies, a $\pi/4$ rotated version of this function was used. This phenomenological response function [Eq. (2)] provides a good description of the data at all energies. The overall strength of the response at a given E is described by the $\mathbf{q}$-averaged or local susceptibility $\chi''(\omega) = \int \chi''(\mathbf{q}, \omega) d^3q / \int d^3q$ determined from the fitted $\chi''(\mathbf{q}, \omega)$.

Figure 3 summarizes the main findings of this work. For $T = 5$ K, Fig. 3(a) shows that $\chi''(\omega)$ is highly structured

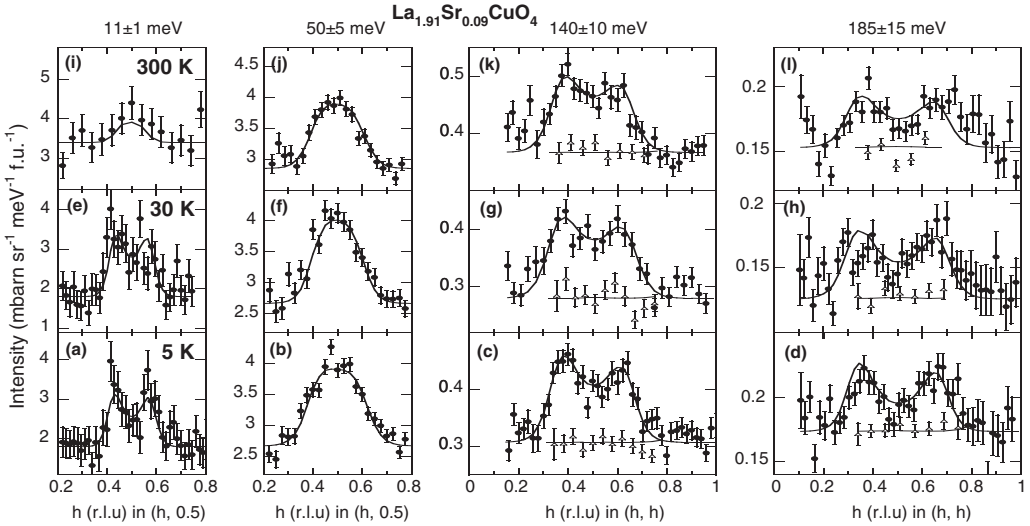

FIG. 2. Constant-E cuts through raw data used to produce the plots in Fig. 1. Data have not been corrected for the Bose or form factors. Solid lines are fits of Eq. (2) convolved with the instrument resolution. Open triangles are background points collected at $(h - 0.35, h + 0.35)$.

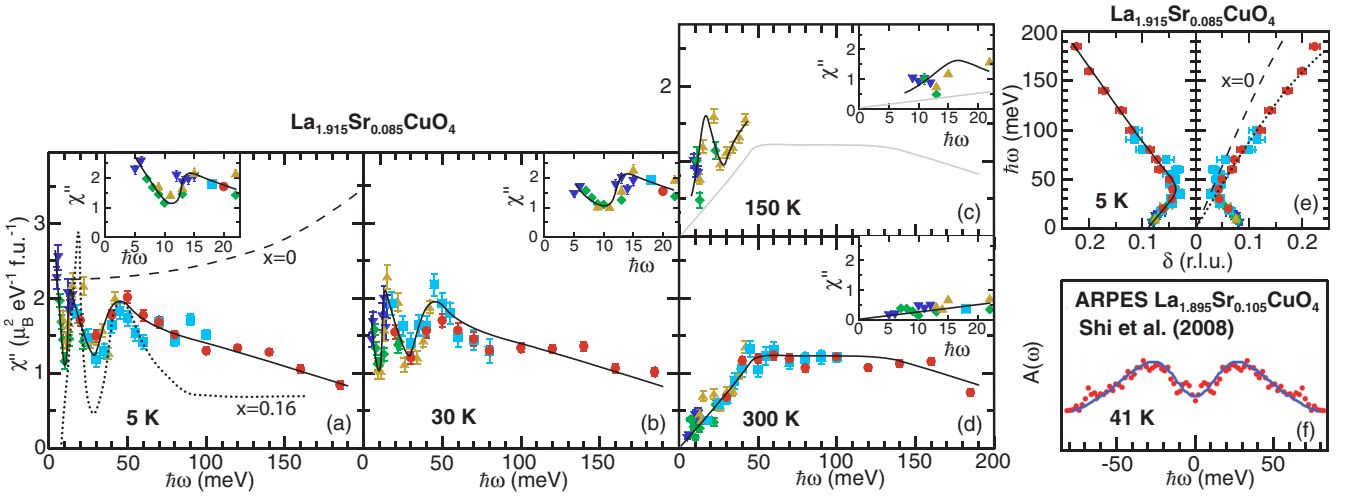

FIG. 3 (color online). (a)–(d) $\chi''(\omega)$ extracted from fitting Eq. (2) to our complete dataset. Insets are expanded views of the low-E region. Symbols indicate E_i: 40 (▼), 55 (◆), 90 (▲), 160 (■), 240 meV (●). Lines are guides to the eye. The dashed and dotted lines in (a) are for $x = 0$ [14] and $x = 0.16$ [9]. Gray line in (c) is a guide from (d). (e) $\delta(\omega)$ for 5 K (30 K is indistinguishable); dashed line is spin-wave dispersion for $x = 0$ [14]; dotted line is fit (see text). (f) Symmetrized ARPES spectral function $A(\omega)$ from Ref. [27]. The peak separation $2\Delta^\star = 51$ meV is a measure of the pseudogap for a sample of slightly higher doping ($x = 0.105$). We expect $2\Delta^\star \approx 60$–70 meV for our sample.

with peaks at 15 and 50 meV. The upturn below 10 meV is due to the freezing of the low-frequency spin fluctuations previously seen by INS [12] and NMR [13] in $La_{2-x}Sr_xCuO_4$ for similar dopings. For $\hbar\omega > 10$ meV, we observe the double-peaked structure seen at optimal doping ($x = 0.16$) [9], with peaks at approximately 15 and 50 meV (compared to 18 and 50 meV for $x = 0.16$). The lower ($E = 15$ meV) peak is due to intensity at the incommensurate (IC) $(1/2, 1/2 \pm \delta)$ and $(1/2 \pm \delta, 1/2)$ positions [see Fig. 1(a)], and the higher ($E = 50$ meV) peak to a resurgent response dispersing from $(1/2, 1/2)$ [see Fig. 1(b)]. The double-peaked structure in $\chi''(\omega)$ is less pronounced for underdoped LSCO ($x = 0.085$) than for the previously measured [9] optimally doped LSCO ($x = 0.16$) [dotted line Fig. 3(a)]. We see a weaker dip near 25 meV and more spectral weight above 50 meV. Our data also give information about the dispersion of the excitations. Figure 3(e) shows the dispersion of $\delta(\omega)$ extracted from our fitting analysis. The form of $\delta(\omega)$ is very similar to that observed at optimal doping with a minimum in $|\delta|$ at about 50 meV. Figures 1(a)–1(d) show maps of $\chi''(\mathbf{q}, \omega)$ for $T = 5$ K at various energies. We observe the same rotation of the four-peaked pattern with E that has been seen in $YBa_2Cu_3O_{6.6}$ [8] and possibly seen in optimally doped $La_{2-x}Sr_xCuO_4$ [9]. The high-E pattern [Figs. 1(c) and 1(d)] is more anisotropic than in optimally doped LSCO [9].

The response in $La_{2-x}Sr_xCuO_4$ ($x = 0.085$) is generally weaker than in La_2CuO_4. The dashed lines in Fig. 3(a) and 3(e) show $\chi''(\omega)$ and $|\delta|$ calculated from Ref. [14]. We may extract an effective exchange constant $J = 87 \pm 4$ by fitting the high-energy ($E > 70$ meV) dispersion to a spin-wave theory. This is substantially less than for La_2CuO_4, where $J = 146 \pm 4$ meV [14]. A quantitatively similar reduction of J with doping has been observed in $YBa_2Cu_3O_{6+x}$ for $x = 0.5$ [8,15,16].

We now discuss the effect of raising T on the magnetic excitations. On increasing T from 5 K to 30 K $\gtrsim T_c$ [Fig. 3(b)], we observe little change in the response except for a small decrease in $\chi''(\omega)$ below 10 meV, as the spin freezing weakens. This is consistent with μSR, NMR [13] and other neutron data [5,17]. On further increasing T to 300 K, $\chi''(\mathbf{q}, \omega)$ changes dramatically over a wide energy range ($0 < E \lesssim 70$ meV). At low-frequencies ($E \approx 5$ meV), $\chi''(\omega)$ is strongly suppressed as low-frequency antiferromagnetic fluctuations or spin freezing disappear. Similar effects are well known in NMR measurements of T_1^{-1} [13,18] which probe $\chi''(\omega)$ at even lower frequencies. Looking over a wider E range, we note that the double-peak structure seen in $\chi''(\omega)$ at 5 K and 30 K disappears on warming to 300 K, leaving a heavily-damped response with a characteristic energy scale of about 50 meV [see Figs. 3(a)–3(d)]. We have limited data at $T = 150$ K [Fig. 3(c)] which show that the $E \approx 15$ meV peak is present but suppressed at this intermediate T. Interestingly, at $T = 300$ K the response is roughly that of the marginal Fermi liquid [19] form, $\chi''(\omega) \sim \tanh(\omega/T)$, postulated to account for the strong T dependence of the electronic properties of the high-T_c superconductors, and previously observed over a much smaller E range in very underdoped $La_{2-x}(Ba, Sr)_xCuO_4$ [3,4].

It is interesting to compare LSCO with other underdoped cuprates. In $YBa_2Cu_3O_{6+x}$ (YBCO) [20,21] the most dramatic change in $\chi''(\mathbf{q}, \omega)$ as T is lowered is the formation of the dispersive "spin resonance mode" which is strongest at $(1/2, 1/2)$. The detailed structure of the low-E

excitations in LSCO is rather different: there appear to be two parts to the response giving rise the a double-peaked structure in $\chi''(\omega)$. The two systems share the common feature that the low-energy excitations become more structured over the energy range 0–60 meV as they move into the pseudogap phase [21]. The stripe ordered material $La_{1.875}Ba_{0.125}CuO_4$ shows very different behavior [22,23]. At low temperatures ($T = 12$ K), this material [22] shows a similar ''hourglass'' dispersion to Fig. 3(e); however, it does not show the double-peaked structure in $\chi''(\omega)$ observed for optimal [9] and underdoped $La_{2-x}Sr_xCuO_4$. Further, on warming from 12 to 300 K, $La_{1.875}Ba_{0.125}CuO_4$ does not show [23] the large and dramatic changes in $\chi''(\omega)$ reported here for $E < 70$ meV in $La_{2-x}Sr_xCuO_4$ ($x = 0.085$). This suggests that the behavior of $La_{1.875}Ba_{0.125}CuO_4$ is due to the magnetic stripe order present for this composition [24].

Many theories have been proposed to describe the magnetic excitations in the cuprates. A large proportion might be broadly divided into two classes: (i) Linear response calculations based on the underlying band structure and the presence of a d-wave energy gap; (ii) theories based on coupled spin ladders which assume phase segregation of the system into undoped antiferromagnetic regions separated by one-dimensional ''stripes'' containing the doped holes. We note that recent calculations [25] of $\chi''(\mathbf{q}, \omega)$ based on linear response theory and band-structure parameters derived from ARPES measurement on underdoped LSCO are able to describe the main features of our $T \leq 30$ K data (i.e., low-E incommensurate peaks; dispersion to a strong commensurate peak; and the rotated anisotropic pattern at high-E).

The present work demonstrates how lowering T from 300 to 30 K can cause dramatic changes in the magnetic response $\chi''(\omega)$ over a wide E range. It is known that the scattering rate for electrons drops abruptly below T_c in high-temperature superconductors. This is seen in many electronic probes including ARPES, conductivity and tunneling. The most natural explanation of this drop is due to the opening of the superconducting gap and the reduction of electron-electron scattering. Surprisingly, this reduction of scattering rate also happens for the underdoped case [1,26], where a ''pseudogap'' (PG) is present above T_c. For the purposes of this discussion, we will define the PG energy such that the effects of the PG are felt below $2\Delta^\star$, when $T < T^\star$. Recent ARPES measurements [27] suggest $2\Delta^\star \approx 60$–70 meV for the $La_{2-x}Sr_xCuO_4$ ($x = 0.085$) studied here [see Fig. 3(f)]. In this Letter, we show that, as the temperature is lowered, the spin excitations become more structured over an energy range $0 < E < 70$ meV which corresponds approximately to $2\Delta^\star$.

There are two general scenarios that could explain the emergence of structured and coherent spin excitations as T is lowered. The first is the concomitant appearance of some form of magnetic order. This explanation in unlikely because only very weak spin freezing or magnetic order is observed for the compositions studied here [12]. Yet the observed $\chi''(\omega)$ has a magnitude comparable with the parent antiferromagnet La_2CuO_4 [14], which has an ordered moment $\approx 0.6\mu_B$. The second scenario is that there is a drop in the damping of the magnetic excitations as we enter the PG state. Thus the magnetic excitations see a drop in damping in a similar way to the electron quasiparticles measured by ARPES and other probes [28].

In conclusion, we have shown that highly structured and coherent magnetic excitations exist at low temperatures ($T \lesssim 30$ K) over a wide energy scale ($5 < E < 200$ meV) in underdoped and superconducting $La_{2-x}Sr_xCuO_4$. At low energies, $E < 70$ meV, we find a double-peaked structure in $\chi''(\omega)$ and a four-peaked structure in wave vector which develop as T is lowered from 300 to 30 K, i.e., as we move into the pseudogap region of the phase diagram. We note that the E scale over which $\chi''(\mathbf{q}, \omega)$ changes most corresponds approximately to the pseudogap energy $2\Delta^\star$ for our sample. The $E \gtrsim 70$ meV excitations do not change significantly with temperature, they are strongly dispersive and $\chi''(\mathbf{q}, \omega)$ shows an anisotropic four-peaked structure which is rotated with respect to lower energies.

We thank A. V. Chubukov and M. R. Norman for useful discussions.

[1] T. Timusk and B. Statt, Rep. Prog. Phys. **62**, 61 (1999).
[2] J. L. Tallon and J. W. Loram, Physica (Amsterdam) **349C**, 53 (2001).
[3] B. Keimer *et al.*, Phys. Rev. Lett. **67**, 1930 (1991).
[4] S. M. Hayden *et al.*, Phys. Rev. Lett. **66**, 821 (1991).
[5] C.-H. Lee *et al.*, J. Phys. Soc. Jpn. **69**, 1170 (2000).
[6] M. Kofu *et al.*, arXiv:0710.5766.
[7] S. Komiya *et al.*, Phys. Rev. B **65**, 214535 (2002).
[8] S. M. Hayden *et al.*, Nature (London) **429**, 531 (2004).
[9] B. Vignolle *et al.*, Nature Phys. **3**, 163 (2007).
[10] O. J. Lipscombe *et al.*, Phys. Rev. Lett. **99**, 067002 (2007).
[11] S. W. Cheong *et al.*, Phys. Rev. Lett. **67**, 1791 (1991).
[12] H. Matsushita *et al.*, J. Phys. Chem. Solids **60**, 1071 (1999).
[13] M.-H. Julien, Physica (Amsterdam) **329–333B**, 693 (2003).
[14] R. Coldea *et al.*, Phys. Rev. Lett. **86**, 5377 (2001).
[15] P. Bourges *et al.*, Phys. Rev. B **56**, R11 439 (1997).
[16] C. Stock *et al.*, Phys. Rev. B **71**, 024522 (2005).
[17] J. Chang *et al.*, Phys. Rev. Lett. **98**, 077004 (2007).
[18] S. Ohsugi *et al.*, J. Phys. Soc. Jpn. **63**, 700 (1994).
[19] C. M. Varma *et al.*, Phys. Rev. Lett. **63**, 1996 (1989).
[20] P. C. Dai *et al.*, Science **284**, 1344 (1999).
[21] V. Hinkov *et al.*, Nature Phys. **3**, 780 (2007).
[22] J. M. Tranquada *et al.*, Nature (London) **429**, 534 (2004).
[23] G. Xu *et al.*, Phys. Rev. B **76**, 014508 (2007).
[24] M. Fujita *et al.*, Phys. Rev. B **70**, 104517 (2004).
[25] M. R. Norman, Phys. Rev. B **75**, 184514 (2007).
[26] K. Takenaka *et al.*, Phys. Rev. B **68**, 134501 (2003).
[27] M. Shi *et al.*, Phys. Rev. Lett. **101**, 047002 (2008).
[28] M. R. Norman *et al.*, Phys. Rev. B **57**, R11 093 (1998).